LITERATURE CITED

1. T.-F. Ho, A. R. McIntosh, and A. C. Weedon, *Can. J. Chem.*, **62**, 967 (1984).
2. J. L. Y. Kong and P. A. Loach, *J. Heterocycl. Chem.*, **17**, 737 (1980).
3. S. Nishitani, N. Kurata, Y. Sakata, S. Misumi, M. Migita, T. Okada, and N. Mataga, *Tetrahedron Lett.*, **22**, 2099 (1981).
4. J. R. Bolton, T.-F. Ho, S. Liauw, A. Siemiarzuk, C. S. K. Wan, and A. C. Weedon, *J. Chem. Soc., Chem. Commun.*, No. 9, 599 (1985).
5. D. Gust and T. Moore, *J. Photochem.*, **29**, 173 (1985).
6. M. Migita, T. Okada, N. Mataga, S. Nishitani, N. Kurata, Y. Sakata, and S. Misumi, *Chem. Phys. Lett.*, **84**, 263 (1981).
7. V. V. Borovkov, E. I. Filippovich, and R. P. Evstigneeva, *Khim. Geterotsikl. Soedin.*, No. 5, 608 (1988).
8. R. P. Evstigneeva, V. V. Borovkov, E. I. Filippovich, and S. I. Sviridov, *Dokl. Akad. Nauk SSSR*, **293**, 1130 (1987).
9. V. V. Borovkov, R. P. Evstigneeva, L. N. Strekova, E. I. Filippovich, and R. F. Khairutdinov, *Usp. Khim.*, **58**, 1032 (1989).
10. V. V. Borovkov and R. P. Evstigneeva, Conference Proceedings FECS of the 5th International Conference on the Chemistry and Biotechnology of Biologically Active Natural Products, Varna, Bulgaria, Vol. 3 (1989), p. 412.
11. G. V. Kirillova, G. V. Ponomarev, V. G. Yashchunskii, and T. A. Babushkina, USSR Author's Certificate No. 857,138; *Byull. Izobret.*, No. 31, 115 (1981).
12. V. V. Borovkov, Master's Dissertation, Moscow Institute of Fine Chemical Technology, Moscow (1988).

EFFECT OF THE pH OF THE MEDIUM ON THE ELECTRONIC ABSORPTION SPECTRA AND STRUCTURE OF 3-METHYL-1-PHENYL-4-PHENYLAZO-5-PYRAZOLONE

B. E. Zaitsev, E. V. Nikiforov, M. A. Ryabov, and G. V. Sheban

UDC 543.422.4.5:547.775

On the basis of the electronic absorption spectra it was found that 3-methyl-1-phenyl-4-phenylazo-5-pyrazolone exists in acidic solutions in mono- and diprotonated forms. It was established by means of calculations by the Pariser—Parr—Pople (PPP) method that in the neutral and protonated forms the quinone hydrazone tautomer of the phenylazopyrazolone is more stable than the azo tautomer, and it was determined that the protonation center is the $N_{(2)}$ atom of the pyrazolone ring. The diprotonated form is most likely the quinone hydrazone tautomer protonated at the heteroring $N_{(2)}$ atom and the α-nitrogen atom of the azo group. In an alkaline medium the phenylazopyrazolone exists in the form of an anion with predominance of the azo form. The effect of substituents ion the diazo component of the phenylazopyrazolone on the long-wave bands of the electronic absorption spectra in various media was explained on the basis of calculation of the distribution of the π-electron density during electron transitions.

3-Methyl-1-phenyl-4-phenylazo-5-pyrazolone (PAP) and its derivatives are used in the textile industry as dyes for fibers and plastics [1]. The results of a study of the structures and properties of these compounds were correlated in [2, 3]. It was found that PAP exists in the form of a quinohydrazone (QH) tautomer in neutral solutions and in the crystalline state [2, 4, 5]. The hydrazone structure of PAP was proved by IR spectroscopy [6], NMR spectroscopy [7], and x-ray diffraction analysis [8]. On the basis of the electronic absorption spectra (EAS) it was concluded that in alkaline media PAP exists in the form of an anion of the azo-OH form (A) [9-11]; the Raman spectroscopic data also indicate an azo enol structure of the PAP anion [12]. At the same time, the EAS and

Patrice Lumumba International-Friendship University, Moscow 117302.

Translated from Khimiya Geterotsiklicheskikh Soedinenii, No. 10, pp. 1331-1336, October, 1991. Original article submitted October 4, 1988; revision submitted December 20, 1990.

0009-3122/91/2710-1064$12.50

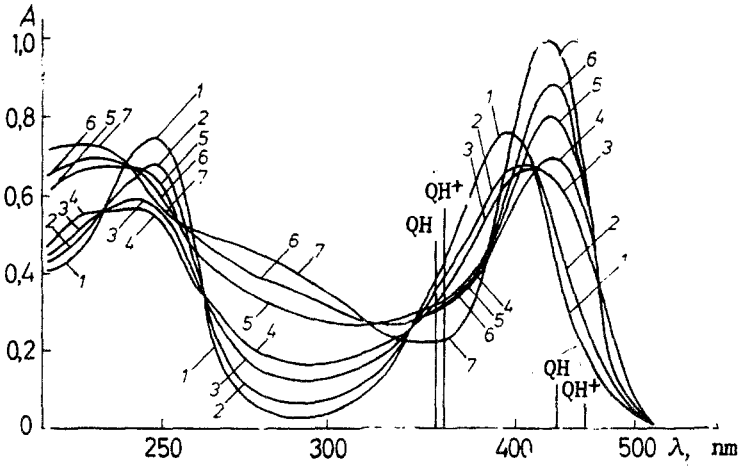

Fig. 1. Experimental and calculated electronic absorption spectra (EAS) of PAP ($c = 3 \cdot 10^{-5}$ mole/liter) in neutral and acidic media for the following H_2SO_4 concentrations: 1) 0%; 2) 17%; 3) 27%; 4) 37%; 5) 57%; 6) 77%; 7) 97%. The vertical lines are the calculated spectra of the hydrazo form (QH) and the $N_{(2)}$-protonated hydrazo form (QH^+).

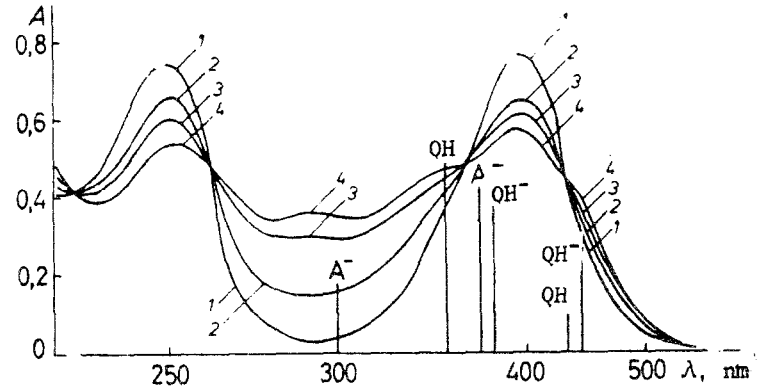

Fig. 2. Experimental and calculated electronic absorption spectra (EAS) of alcohol solutions of PAP ($c = 3 \cdot 10^{-5}$ mole/liter) in neutral and alkaline media: 1) pH 7.20; 2) pH 8.85; 3) pH 11.20; 4) pH 13.40. The vertical lines are the calculated spectra of the hydrazo form (QH), the anion of the hydrazo form (QH^-), and the anion of the azo form (A^-).

structure of PAP in acidic media have not been adequately studied: quantum-chemical calculations have been made only for the neutral and anionic forms [5, 10] and are not available for the protonated forms; a bathochromic shift of the long-wave band (LB) in the EAS upon protonation of PAP has been ascertained [6], but the structure of the cation and the spectral data have not been discussed. Moreover, the literature does not contain an interpretation of the EAS of PAP in acidic and alkaline media that draws upon the calculated data. In this connection the present research was devoted to a study of the structure and electronic absorption spectra of PAP in acidic, neutral, and alkaline media.

A broad long-wave band with λ_{max} 394 nm (the half width of the band is 110 nm) and ε $2.5 \cdot 10^4$ liters/mole·cm, which corresponds to the absorption of the neutral form of PAP, is observed in the EAS of PAP in aqueous ethanol solution (see Fig. 1, curve 1). When the sulfuric acid concentration in solution is increased, four isobestic points (408, 336, 266, and 236 nm), which attest to the existence of neutral and monoprotonated forms in solution and correspond to the first step of protonation, are observed in the spectra. The long-wave band of the monoprotonated form is characterized by λ_{max} 428 nm and ε $2.3 \cdot 10^4$ (Fig. 1, curve 4). With a further increase in the H_2SO_4 concentration the isobestic points corresponding to monoprotonation vanish, and four new isobestic points (387, 320, 257, and 246 nm), which correspond to diprotonation of PAP, appear. For the long-wave band of the diprotonated form of PAP λ_{max} is 424 nm and ε is $3.3 \cdot 10^4$ (Fig. 1, curve 7). The pK values of the mono- and diprotonated forms of PAP are -2.94 and -8.26, respectively.

TABLE 1. Energies of Atomization (ΔH) and Coefficients of Solvation (M) of the Ionic Forms of Hydrazo and Azo Tautomers of PAP

Ionic charge	Protonation site	XГ		A	
		ΔH, eV	M, eV	ΔH, eV	M, eV
−1	—	176,31	4,70	175,38	2,31
0	—	179,35	3,60	179,84	2,46
+1	$N_{(2)}$	184,48	4,83	185,09	3,64
+1	$N_{(7)}$	183,87	4,00	184,07	2,71
+1	$N_{(8)}$	182,29	2,87	184,43	3,34
+1	$N_{(1)}$	182,43	2,91	—	—

TABLE 2. Characteristics of the Long-Wave Bands of the Electronic Absorption Spectra (EAS) of the Ionic Forms of the Hydrazo and Azo Tautomers of PAP*

Ionic charge	λ^e_{max}, nm	$\varepsilon^e \times 10^{-4}$	QH				A			
			λ_1^p, nm	f_1^p	λ_2^p, нм	f_2^p	λ_1^p, nm	f_1^p	λ_2^p, nm	f_2^p
−1	386	2,1	439	0,52	378	0,96	368	0,98	301	0,39
0	394	2,5	428	0,20	352	0,93	358	1,18	293	0,17
+1**	428	2,3	454	0,09	358	1,01	355	1,25	281	0,17
+2**	424	3,3	547	0,07	410	1,03	—	—	—	—

*Symbols: λ_{max}^e is the experimental value of the wavelength of the long-wave band, ε^e is the experimental value of its coefficient of extinction, λ^c is the calculated value of the wavelength, and f^c is the oscillator for of the first two electron transitions for the ionic forms of the QH and A tautomers.

**Monoprotonation takes place at the $N_{(2)}$ atom, while diprotonation takes place at the $N_{(2)}$ and $N_{(7)}$ atoms.

TABLE 3. Changes in the π Charges of the Atoms (ΔQ_1 and ΔQ_2 and Electron Charge) of The Various Forms of PAP for the First Two Electron Transitions

Atom	A		QH^-		QH		QH^{+*}		QH^{2+**}	
	ΔQ_1	ΔQ_2	ΔQ_1	ΔQ_2	ΔQ_1	ΔQ_2	ΔQ_1	ΔQ_2	ΔQ_1	ΔQ_2
A***	−0,03	0,05	0,12	0,16	0,23	0,09	0,32	0,05	0,35	0,03
$N_{(1)}$	−0,01	0,19	0,14	0,13	0,22	0,04	0,29	0,02	0,30	0,01
$N_{(2)}$	0,08	0,15	0,11	−0,04	0,07	−0,05	0,02	−0,03	0,01	−0,03
$C_{(3)}$	−0,01	0,11	−0,02	0,03	0,00	−0,04	−0,10	−0,09	−0,08	−0,08
$C_{(9)}$	0,00	0,03	0,00	0,01	0,01	0,00	−0,01	−0,01	−0,01	−0,01
$C_{(4)}$	0,28	0,01	−0,05	0,05	−0,15	−0,02	−0,16	0,00	−0,23	−0,08
$C_{(5)}$	−0,09	−0,18	−0,04	−0,08	−0,06	−0,09	−0,04	−0,06	−0,04	−0,05
$O_{(6)}$	0,09	0,05	0,14	−0,08	0,10	−0,09	0,15	−0,06	0,11	−0,07
$N_{(7)}$	−0,26	−0,18	−0,27	−0,26	−0,31	−0,30	−0,32	−0,31	−0,24	−0,24
$N_{(8)}$	−0,04	−0,15	0,00	0,09	−0,05	0,15	−0,08	0,17	−0,10	0,16
B***	−0,01	−0,08	−0,13	−0,01	−0,06	0,31	−0,07	0,32	−0,07	0,36

*QH^+ is the monoprotonated [at the $N_{(2)}$ atom] QH tautomer.

**QH^{2+} is the diprotonated [at the $N_{(2)}$ and $N_{(7)}$ atoms] QH tautomer.

***The overall change in the charges of the atoms of benzene rings A and B is presented.

When the pH of an ethanol solution of PAP is increased, one observes a decrease in the intensity and a small hypsochromic shift of the long-wave band; isobestic points (426, 360, 265, and 229 nm) corresponding to deprotonated PAP are observed (see Fig. 2). The long-wave band of the anionic form of PAP is characterized by λ_{max} 386 nm and ε $2.1 \cdot 10^4$ (see Fig. 2, curve 4). Thus the electronic spectra provide evidence that PAP exists in solutions in the form of anionic, neutral, and mono- and diprotonated forms, depending on the pH of the medium.

To determine the structures of the various forms of PAP by the Pariser—Parr—Pople (PPP) method we calculated the anionic, neutral, and several protonated forms of the QH and A tautomers. The numbering of the atoms and the designation of the fragments of the molecule are given in the structural formulas:

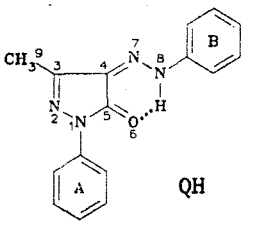

QH

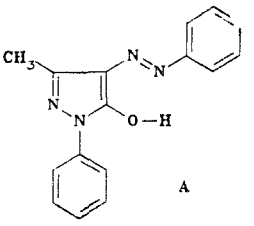

A

The atomization energies ΔH and the coefficients of solvation M were calculated (see Table 1). It is apparent from the values presented for the neutral forms of PAP that in the gas phase the azo tautomer should be more stable than the hydrazone tautomer. However, on passing to solutions, i.e., taking into account the energy of solvation $E = M(1 - 1/\varepsilon)$, where ε is the dielectric permeability of the solvent, the QH tautomer proves to be more stable. Since this is in agreement with the experimental results, it may be hoped that the calculations will also prove to be accurate in the study of the structures of the charged forms of PAP. It follows from the ΔH and M data for the monoprotonated forms of PAP (see Table 1) that the QH tautomer that is protonated at the $N_{(2)}$ atom of the pyrazolone ring is the most stable form in solution. The second [after the $N_{(2)}$ atom] energically favorable protonation center is the $N_{(7)}$ atom of the azo group, and it may therefore be assumed that the diprotonated form of PAP is the tautomer protonated at the $N_{(2)}$ and $N_{(7)}$ atoms that we calculated.

As regards the deprotonated forms of PAP, the calculated (by us) anions of the QH and A tautomers are boundary resonance structures of the same anion. Their comparison makes it possible to evaluate the contribution of each of the boundary structures to the actually observed structure. Thus, according to the ΔH and M values presented in Table 1, the QH structure should make a large contribution.

The choice between the tautomeric structures of one or another ionic form on the basis of the energy criterion can be supplemented by comparison of the experimental and calculated parameters of the electron transitions (see Table 2).

The calculated EAS of the QH tautomer contain two long-wave transitions at 428 and 352 nm. The 428 nm value lies on the long-wave side, while the 352 nm value lies on the short-wave side of the broad experimental band (see Fig. 1) with λ_{max} 394 nm. The observed band is probably complex and is the combination of the two calculated transitions. It should be noted that for both the QH tautomer and for all of the remaining calculated molecules the first electron transition is due, by a factor of more than 90%, to transition from the highest occupied molecular orbital (HOMO) to the lowest vacant molecular orbital (LVMO), while the second transition is primarily due to transition from the second HOMO to the LVMO.

The calculated EAS of the hydrazo tautomer protonated at the $N_{(2)}$ atom (QH^+) is characterized in the long-wave region by transitions at 454 and 358 nm. A broad absorption band with λ_{max} 428 nm and a band half width of 102 nm is experimentally observed (see Fig. 1). The large half width of the experimental band can be explained by overlapping of the calculated bands at 454 and 358 nm.

It is apparent from the data in Table 2 that the calculated parameters of the long-wave bands of the EAS of the neutral and monoprotonated [at the $N_{(2)}$ atom] azo tautomer are in poorer agreement with the experimental values than the calculated spectra of the QH tautomer.

The calculated EAS of the QH tautomer diprotonated at the $N_{(2)}$ and $N_{(7)}$ atoms has two long-wave transitions — 547 and 410 nm. The experimental spectrum contains an intense absorption band at 424 nm. Since the oscillator force of the transition at 410 nm is considerably greater than for the transition at 547 nm (see Table 2), the experimental band evidently contains a greater contribution from the band at 410 nm than from the band at 547 nm.

A comparison of the experimental extinction coefficients and the calculated oscillator forces for the electron transitions shows that there this no quantitative correlation between them and that one can only speak of a qualitative agreement between them. According to the data in Table 2, λ_1, λ_2, and f_2 increase with an increase in the positive charge of the QH tautomer, while f_1 decreases. The experimentally observed bathochromic shift upon monoprotonation indicates retention of the appreciable contribution of λ_1, while the decrease in f_1 predetermines a

decrease in ε^e. The hypsochromic shift of the long-wave band upon diprotonation indicates an increase in the contribution of λ_2, while the greater f_2 value corresponds to an increase in extinction coefficient ε (see Table 2).

Calculation of the EAS of the anionic forms of PAP gives bands at 439 and 378 nm in the case of the QH anion and at 368 and 301 nm in the case of the azo anion (see Table 2). Since the half width of the experimental band at 386 nm is large (see Fig. 2), it may be assumed that the actual anion contains contributions from both resonance forms. It follows from the data in Table 2 that λ_1^c, λ_2^c, f_1^c, and f_2^c increase upon deprotonation of the QH tautomer, i.e., a bathochromic shift and an increase in the intensity of the absorption band should be observed in the formation of the QH anion. However, the experimental pattern is the opposite: the absorption band is shifted hypsochromically, while its intensity decreases. This sort of character of the change in the EAS of PAP upon deprotonation can be explained by the existence in the anionic form of PAP of a large contribution of the azo-anionic resonance structure, the absorption bands of which are shifted to the short-wave region relative to the bands of the QH anion (see Table 2).

The changes in the π-electron charges of the atoms (ΔQ_1 and ΔQ_2) for the first and second electron transitions, respectively, were calculated (see Table 3). It is apparent that an increase in the π-electron density on the azo group is observed in each transition for all of the molecules; this constitutes evidence for a large contribution of the π AO of the azo group to the LVMO. However, the redistribution of the electron density upon excitation in the remainder of the molecule may be different. Thus a shift of the π-electron density from the $AN_{(1)}$ fragment to the $C_{(4)}$ and $N_{(7)}$ atoms occurs for the neutral QH tautomer during the first electron transition; during the second electron transition the electron density is redistributed in the opposite direction — from the $BN_{(8)}$ fragment to the $N_{(7)}Pz$ fragment (see Table 3). Similar character of the redistribution of the electron density is observed of the monoprotonated [at the $N_{(2)}$ atom] and the diprotonated [at the $N_{(2)}$ and $N_{(7)}$ atoms] QH tautomers. In view of the fact that the oscillator force of the second electron transition f_2 is much greater than f_1 for the first transition (see Table 2), it may be assumed that the resulting redistribution of the electron density corresponding to the actually observed transition will occur in the direction from $BN_{(8)}$ to $N_{(7)}Pz$.

A different pattern is observed for the anionic forms of PAP. In the case of the anionic form of the QH tautomer for the first electron transition the π-electron density is shifted from the $AN_{(1)}N_{(2)}O_{(6)}$ fragment to $BN_{(7)}$. Redistribution of the electron density from the $AN_{(1)}$ fragment to the $N_{(7)}$ atom occurs during the second electron transition, while the $N_{(8)}$ atom and the $N_{(8)}B$ fragment as a whole are a weak donor here (see Table 3). In the case of the azo-anionic form in the first transition the electron density is shifted from the $N_{(2)}C_{(4)}$ fragment to the $N_{(7)}N_{(8)}$ fragment, whereas in the second transition it is shifted from the $AN_{(1)}N_{(2)}C_{(3)}$ fragment to the $N_{(7)}N_{(8)}B$ fragment. According to the f values, the first transition for the azo anion [0.31 of the electron charge is transferred to the $N_{(7)}N_{(8)}B$ fragment] and the second transition for the QH anion [only 0.18 of the electron charge is transferred to the $N_{(7)}N_{(8)}B$ fragment] are the most intensive. Hence, it may be assumed that in the electron transition the PAP anion that contains contributions of both resonance structures the electron density will be shifted from the pyrazolone ring to the azo group and phenyl ring B; the transfer of electron density to the $N_{(7)}N_{(8)}B$ fragment will be more significant, the greater the contribution of the azo-anionic form to the actual structure.

The experimentally found opposite (in direction) redistribution of the π-electron density in the electron transitions in neutral and protonated PAP, on the one hand, and in the PAP anion, on the other, makes it possible to explain the shift of the long-wave bands of the EAS of PAP in various media when electron-donor and electron-acceptor substituents are introduced into phenyl ring B.

In [11] it was found that the maximum bathochromic shift is observed in a neutral medium for donor substituents, whereas the maximum bathochromic shift is observed in an alkaline medium for acceptor substituents. For example, in ethanol the λ_{max} values of the long-wave bands of the EAS of PAP with $N(C_2H_5)_2$, NH_2, H, CN, and NO_2 groups in the para position of phenyl ring B are, respectively, 500, 474, 398, 382, and 397 nm in a neutral medium and 435 and 403 (for this compound and the next compound two maxima of the long-wave band were found), 424 and 391, 375, 439, and 493 nm in an alkaline medium. In our research we found that during an electron transition the π-electron density is shifted from $BN_{(8)}$ to $N_{(7)}Pz$ in the case of neutral and protonated PAP and from Pz to $N_{(7)}H_{(8)}B$ in the case of the anionic form of PAP. Thus if the redistributions of the π-electron density when substituents are introduced and during electron transitions coincide with respect to direction, this leads to a bathochromic shift of the long-wave band. If, however, these shifts are opposite in direction, this does not lead to a significant shift of the long-wave band.

EXPERIMENTAL

3-Methyl-1-phenyl-4-phenylazo-5-pyrazolone was recrystallized from benzene. The electronic absorption spectra (EAS) were recorded with a Specord UV-vis spectrophotometer at 200-700 nm. The investigation of the protonation of PAP was carried out in an aqueous ethanol mixture. The C_2H_5OH concentration was constant (3% by volume). The H_2O and H_2SO_4 concentrations ranged from 97% to 0% by volume. The calculations of the pK values of the monoprotonated (pK^I) and diprotonated (pK^{II}) forms of PAP were carried out spectrophotometrically

[13]. The analytical wavelength for the determination of pK^{I} was 428 nm, while the analytical wavelength for the determination of pK^{II} was 424 nm. To record the spectrum of the neutral form we prepared a solution of PAP in a mixture of 3% C_2H_5OH and 97% H_2O; for the monoprotonated form we used 60% H_2O and 37% H_2SO_4, while for the diprotonated form we used 97% H_2SO_4. The measurements were made at 20-25°C. The deprotonation of PAP was studied in an ethanol medium with the addition of NaOH. The quantum-chemical calculations of the azo and hydrazone tautomers of PAP, as well as their protonated and deprotonated forms, were made by the Pariser—Parr—Pople (PPP) method with optimization of the interatomic distances with respect to the minimum of the heats of atomization [14].

LITERATURE CITED

1. B. I. Stepanov, *Introduction to the Chemistry and Technology of Organic Dyes* [in Russian], Khimiya, Moscow (1984).
2. J. Elguero, C. Marzin, A. R. Katritzky, and P. Linda, *The Tautomerism of Heterocycles*, Academic Press, New York—London (1976), p. 336.
3. K. A. Hafez, E. M. Kayed, and K. U. Sadek, *J. Heterocycl. Chem.*, **22**, 241 (1985).
4. J. Elguero, R. Jacquier, and G. Tarrago, *Bull. Soc. Chim. France*, No. 9, 2990 (1966).
5. J. Arriau, J. P. Campillo, J. Elguero, and J. M. Pereillo, *Tetrahedron*, **30**, 1345 (1974).
6. B. E. Zaitsev, V. A. Zaitseva, A. K. Molodkin, and E. S. Obraztsova, *Zh. Neorg. Khim.*, **24**, 127 (1979).
7. A. Lycka and D. Snobl, *Coll. Czech. Chem. Commun.*, **42**, 892 (1981).
8. L. G. Kuz'mina, L. P. Grigor'eva, Yu. T. Struchkov, Z. I. Ezhkova, B. E. Zaitsev, V. A. Zaitseva, and P. P. Pron'kin, *Khim. Geterotsikl. Soedin.*, No. 6, 816 (1985).
9. I. S. Ioffe, L. M. Kryukova, and L. Yu. Kim, *Zh. Org. Khim.*, 7, 2193 (1971).
10. D. Simov, S. Stoyanov, and S. Tomov, *Godishnik Sofiisk. Univ. "Kliment Okhridski": Khim. Fak.*, **74**, 155 (1979/1980).
11. P. Nikolov, P. Fratev, S. Stoyanov, and O. E. Polanskii (Polansky), *Z. Naturforsch.*, **36A**, 191 (1981).
12. J. J. Trotter, *Appl. Spectr.*, **31**, 30 (1977).
13. A. Albert and E. Sergeant, *Ionization Constants of Acids and Bases* [Russian translation], Khimiya, Moscow—Leningrad (1964).
14. M. Dewar, *Molecular Orbital Theory in Organic Chemistry* [Russian translation], Mir, Moscow (1972), p. 464.